Molecular Cell *21*, 331–336, February 3, 2006 ©2006 Elsevier Inc. DOI 10.1016/j.molcel.2005.12.015

Full-Length Myosin VI Dimerizes and Moves Processively along Actin Filaments upon Monomer Clustering

Hyokeun Park,[1,7] Bhagavathi Ramamurthy,[4,7] Mirko Travaglia,[5] Dan Safer,[4] Li-Qiong Chen,[4] Clara Franzini-Armstrong,[5,6] Paul R. Selvin,[2,3,*] and H. Lee Sweeney[4,6,*]

[1] Department of Chemistry
[2] Department of Physics
[3] Center for Biophysics and Computational Biology
University of Illinois
Urbana, Illinois 61801
[4] Department of Physiology
[5] Department of Cell and Developmental Biology
[6] Pennsylvania Muscle Institute
University of Pennsylvania School of Medicine
3700 Hamilton Walk
Philadelphia, Pennsylvania 19104

Summary

Myosin VI is a reverse direction actin-based motor capable of taking large steps (30–36 nm) when dimerized. However, all dimeric myosin VI molecules so far examined have included nonnative coiled-coil sequences, and reports on full-length myosin VI have failed to demonstrate the existence of dimers. Herein, we demonstrate that full-length myosin VI is capable of forming stable, processive dimers when monomers are clustered, which move up to 1–2 μm in ~30 nm, hand-over-hand steps. Furthermore, we present data consistent with the monomers being prevented from dimerizing unless they are held in close proximity and that dimerization is somewhat inhibited by the cargo binding tail. A model thus emerges that cargo binding likely clusters and initiates dimerization of full-length myosin VI molecules. Although this mechanism has not been previously described for members of the myosin superfamily, it is somewhat analogous to the proposed mechanism of dimerization for the kinesin *Unc104*.

Introduction

Class VI myosins were the first of the myosin superfamily identified to traffic toward the pointed (−) end of the actin filament (Wells et al., 1999). In addition to their singular directionality, myosin VI has a number of additional unusual features. For example, even though single molecules of two-headed myosin VI, like myosin V, are capable of taking multiple steps (processive movement) on an actin filament without detachment (Wells et al., 1999; Kellerman and Miller, 1992), myosin VI has only a short "lever arm" with one calmodulin (Hasson and Mooseker, 1994). One possible explanation is that the lever arm may be extended in the dimer via a somewhat flexible region distal to the calmodulin (Rock et al., 2005). There is also a second calmodulin bound to one of two unique myosin VI inserts (Bahloul et al., 2004; Ménétrey et al., 2005). This calmodulin is structural, contains four tightly bound calcium ions, and is not exchangeable.

Although myosin VI contains a sequence that is predicted to form a coiled coil with high probability (Rock et al., 2005), so far dimerization has only been observed after insertion of a nonnative coiled-coil sequence distal to the predicted coiled-coil region (Rock et al., 2001; Nishikawa et al., 2002). It was recently suggested that for a number of myosin superfamily members, including myosin VI, the predicted coiled-coil region is in fact a stable single α helix incapable of coiled-coil dimerization (Knight et al., 2005). Indeed, it has been reported that full-length myosin VI does not form dimers (Lister et al., 2004). However, we previously proposed that the properties of the artificially dimerized myosin VI motor (gating and step size) suggest that the protein may be a functional dimer in situ (De La Cruz et al., 2001; Rock et al., 2001; Yildiz et al., 2004), even if the isolated full-length protein is monomeric (Rock et al., 2005). To account for this apparent discrepancy, we postulated that myosin VI may undergo cargo-mediated dimerization, as has been proposed for the kinesin *Unc104* (Al-Bassam et al., 2003). There are at least two possibilities of how this could occur. The first is that the coiled-coil region of myosin VI may be capable of initiating dimerization but is prevented from doing so by interactions with other sequences within the molecule. In the case of *Unc104*, the proposed mechanism is the formation of an antiparallel coiled coil within the full-length protein that prevents dimerization unless the molecule binds to its cargo. The second possibility is that the coiled-coil region of myosin VI is capable of dimerization but is incapable of initiating dimerization. In this case, binding to cargo could allow interactions that would eventually induce dimerization. We now demonstrate that in the case of myosin VI, the predicted region of coiled coil can lead to dimerization. However the dimerization is not self-initiated but requires some means of bringing two monomers together, as can be done in vitro, by a temporary attachment to actin filaments or binding to an antibody.

Results

Myosin VI Truncations to Assess Regions Capable of Dimerization

In order to dissect the myosin VI domain that may allow dimerization under appropriate conditions, we created a number of truncations of the full-length myosin VI (MVI-1273), as depicted in Figure 1. These truncations sequentially removed the putative cargo binding domain, which contains all of the sequences reported to bind to identified myosin VI partners (MVI-1050), then the remaining sequence, up to the putative coiled coil (MVI-992), followed by the removal of the highest probability coiled coil (MVI-917), and finally removal of all predicted coiled coil (MVI-839 or S1). All constructs, other than the full length, had a Flag epitope appended to the

*Correspondence: selvin@uiuc.edu (P.R.S.); lsweeney@mail.med.upenn.edu (H.L.S.)
[7] These authors contributed equally to this work.

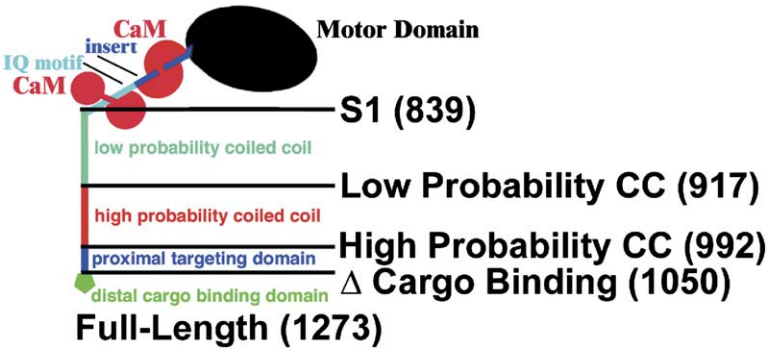

Figure 1. Schematic of Myosin VI Constructs

The full-length myosin VI molecule is diagramed along with the sites of truncations for this study (noted by the C-terminal amino acid number). The N-terminal motor domain is followed by a unique insert that binds the structural CaM, followed by an exchangeable CaM that is bound to an IQ motif. This is followed by a region of low probability coiled coil that may form an extension of the lever arm formed by the bound CaMs. This is followed by a region of predicted high probability coiled coil, which we show to be necessary for dimerization. We hypothesize that the proximal portion of cargo binding domain may form an extension, allowing the cargo binding domain to fold back and inhibit dimerization when not bound to cargo.

C terminus to allow purification and antibody clustering of the tails. Attempts to place a C-terminal tag on the full-length construct interfered with protein production and function. Data from these constructs were compared with those obtained from an MVI "zippered" dimer constructed by the insertion of a leucine zipper (GCN4 coiled coil; Lumb et al. [1994] and see Rock et al. [2001, 2005]).

Initiation of Dimerization

Two types of induced-dimerization protocols were developed. The first involved saturated decoration of actin filaments in the absence of nucleotide. The densely packed molecules were then released from actin by the addition of ATP and assayed. The second type of initiated dimerization involved saturation of anti-Flag antibody with the C-terminal Flag containing myosin VI constructs, thus positioning the C termini of two molecules in close proximity. The molecules were released from antibody via competition with excess Flag peptide, and antibody was removed by protein A-conjugated beads. Assays were performed within a few hours of release of myosin VI from the antibody or from actin. This was done because preliminary studies revealed that dimers so formed were only stable on the order of hours.

Assays of Dimerization

Formation of myosin VI dimers was examined directly by the use of rotary shadowing electron microscopy (EM) and indirectly by two types of functional assays of dimerization. The first assay was actin-activated ATPase activity. This assay took advantage of the previous data from zippered dimers (De La Cruz et al., 2001; Morris et al., 2003) demonstrating that the activity of the dimer is roughly half that per head of the monomer (i.e., myosin VI dimers show gating of activity of the heads). The second assay applied the same technique that was developed and used to demonstrate a hand-over-hand mechanism for myosin V and myosin VI motility (Yildiz et al., 2003, 2004; Okten et al., 2004). This technique has been termed *f*luorescence *i*maging with *o*ne *n*anometer *a*ccuracy (FIONA) and can track the position of a single fluorophore with ~1.5 nm resolution. For this assay, ~15%–20% of the monomeric heads were labeled by placing a fluorophore on the IQ bound calmodulin before the molecule was bound to actin filaments. Thus, if dimerization took place, only at most one head of any dimer would be labeled (the majority of the molecules would not contain labeled heads). Dimerization would be indicated by hand-over-hand steps of ~30 nm in the presence of ATP (as for the zippered dimer), which would be observed as displacements of ~60 nm of the single-labeled head. Monomeric myosin VI would be expected to simply dissociate from actin upon addition of ATP.

ATPase Assays Are Consistent with Dimer Formation via Predicted Coiled Coil

As shown in Table 1, in the absence of attempts to induce dimerization, the extrapolated V_{max} of the actin-activated ATPase activities was essentially the same for all constructs shown in Figure 1 and was equivalent to the activity of the single-headed myosin VI construct. After the initiated dimerization procedures, the two constructs containing the predicted high probability coiled-coil region, but with the cargo binding region deleted,

Table 1. Actin-Activated ATPase Activity (V_{max}) of Myosin VI Constructs

Construct	V_{max} (Head^{-1}Second^{-1})	After Antibody Binding V_{max} (Head^{-1}Second^{-1})	After Actin Saturation V_{max} (Head^{-1}Second^{-1})
S1 (MVI-839)	5.9 ± 1.1	6.0 ± 1.2	5.7 ± 0.9
MVI-917	6.0 ± 1.3	6.4 ± 1.5	5.6 ± 1.3
MVI-992	7.1 ± 1.6	2.5 ± 1.7	2.9 ± 0.8
MVI-1050	4.8 ± 1.9	2.2 ± 0.3	2.0 ± 0.4
Full length	4.5 ± 1.4	NA	4.5 ± 0.8
Zippered dimer	2.4 ± 0.8	2.5 ± 1.1	2.4 ± 1.3

Mean values (±SD) of three to four independent protein preparations are shown for each construct and condition.

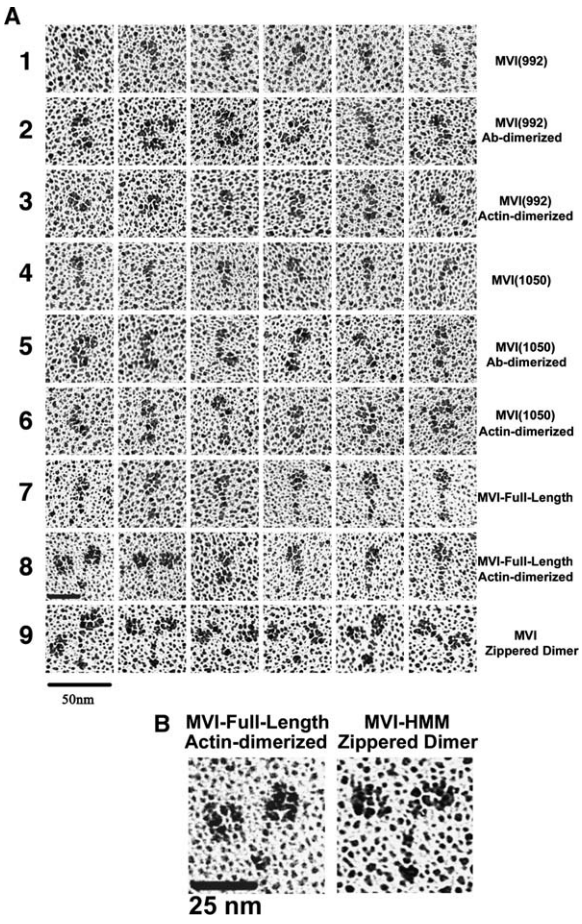

Figure 2. Rotary Shadowing EM of Myosin VI Constructs

Representative images for each myosin VI construct and condition are shown. Monomeric myosin VI ([A], rows 1, 4, and 7) shows a single globular motor domain and a narrow lever arm. The latter is not always clearly visible, particularly in the truncated molecules. After dimer-inducing treatments (association either with actin or an antibody, Ab), dimers are detected. These dimers show two closely spaced motor domains and an intervening link. Note that the dimers from truncated constructs (MVI-992 and MVI-1050, [A], rows 2 and 3 and 5 and 6) appear to collapse on the substrate more than those from the full-length MVI ([A], row 8). Also note that few dimers were found in the actin-dimerized full-length MVI ([A], row 8, see Table 2). The two images at higher magnification (B) compare full-length and zippered dimers (see text). The stalk is longer and more obvious in the latter.

showed activity consistent with dimer formation (half the activity per head of the monomer). The full-length construct had actin-activated ATPase activity consistent with a monomer even after initiated dimerization by binding to actin. The construct missing the high probability coiled coil, but containing the low probability coiled-coil (MVI-917) and the construct truncated after the IQ motif (S1, MVI-839), showed monomer-like activity after clustering by either antibody or actin binding.

Rotary Shadowing EM Directly Demonstrates Formation of Native Dimers

EM (Figure 2 and Table 2), before and after initiated dimerization protocols, led to the same general conclusions. Namely, that either clustering procedure induced dimerization of high proportions of the constructs containing the predicted high probability coiled coil, but with the cargo binding domain removed. (Note that although a small number of molecules were scored as dimers for the truncated myosin VI constructs in the absence of initiating dimerization [Table 2], these small numbers were not statistically significant. It is likely that these were monomers that randomly settled near each other and thus scored as dimers.) Antibody-initiated dimerization could not be performed on the full-length molecules, but after binding and release from actin, about 17% of the EM profiles appeared as dimers. Even though the frequency of dimers is small, it is statistically significant (Table 2), and indeed, a similar number of dimers was detected by single molecule functional assays (FIONA, see below). ATPase assays, however, could not detect the presence of dimers within this sample.

Table 2. Myosin VI Constructs as Assessed by Rotary Shadowing EM

Construct	Percentage of Dimers	Percentage of Dimers after Antibody Binding	Percentage of Dimers after Actin Saturation
S1 (MVI-839)	NS (5 ± 4)	NS (8 ± 5)	NS (10 ± 10)
MVI-917	NS (8 ± 2)	NS (9 ± 6)	NS (1 ± 1)
MVI-992	NS (7 ± 4)	78 ± 17[a]	52 ± 10[a]
MVI-1050	NS (4 ± 5)	61 ± 9[a]	70 ± 9[a]
Full length	0 ± 0	NA	17 ± 2[a]
Zippered dimer	100 ± 0	ND	ND

Mean ± SD. For each construct and condition, data were obtained from a single spray experiment; two to five electron micrographs and a total of 105–512 molecules (56 and 76 molecules for MVI-992 and 76 for MVI-917, both after antibody clustering). Abbreviations: NS, a small number of objects were scored as dimers but were not statistically significant; ND, protocol could not be performed. Student's t test with confidence at 5%. The following populations are significantly different: MVI-992/MVI-992 antibody $p < 4*10^{-3}$; MVI-992/MVI-992 actin $p < 8.5*10^{-5}$; MVI-1050/MVI-1050 actin $p < 1.4*10^{-3}$; MVI-1050/MVI-1050 antibody $p < 7*10^{-4}$; and full-length/full-length actin $p < 6.\ 10^{-3}$. The following populations are not significantly different: MVI-839/MVI-917 p = 0.6; MVI-839/MVI-992 p = 0.8; MVI-839/MVI-1050 p = 0.8; MVI-992/MVI-1050 p = 0.5; MVI-839/full-length actin p = 0.2; MVI-839/MVI-839 antibody p = 0.6; MVI-839/MVI-839 actin p = 0.6; MVI-917/MVI-917 antibody p = 0.8; and MVI-917/MVI-917 actin p = 0.05.
[a] Significant number of dimers detected.

Results from the ATPase assays and EM suggest that even when the molecules are physically brought together, dimerization is not easily initiated. Interestingly, the efficiency of dimerization was similar whether the molecules were held close together by either their C termini (antibody) or N termini (actin). Furthermore, the few full-length dimers that we observed were unusual in appearance as compared to the zippered dimer (Figure 2B), in that the stalk, which is contributed by the coiled coil and is seen in shadowed images as a straight segment, is clearly visible in the zippered dimers, but not in rigor binding-induced dimers of the native molecule.

Native Dimers Move Processively

To assess whether or not the native dimers function as processive motors, single molecule assays (FIONA) were performed with a slight modification of the actin-initiated dimerization procedure. In this case, myosin

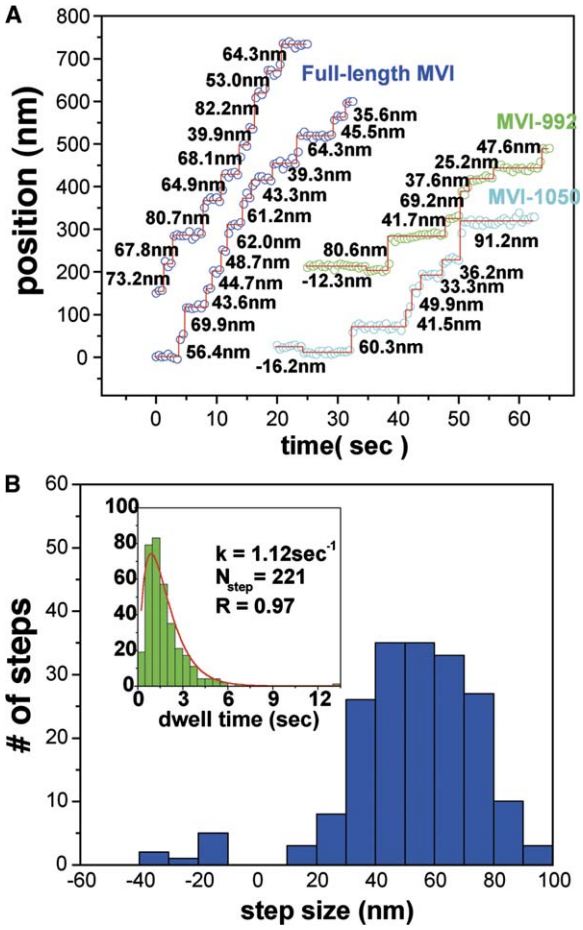

Figure 3. Stepping of Cy3-Labeled Full-Length and Mutant Myosin VI after Rigor Binding to Initiate Dimerization

(A) A subset of the myosin VI molecules was labeled on the IQ bound calmodulin with Cy3. The hand-over-hand characteristics of full-length myosin VI (blue circles), MVI-992 (green circle), and MVI-1050 (cyan circle) are clearly shown, as the traces for the labeled head showed ~60 nm steps. For the full-length myosin VI, the average forward step size was 55.2 ± 17.2 nm (n = 180), which is almost double the average center of mass (~30 nm) of myosin VI. The average backward step size of full-length myosin VI was −20.4 ± 8.3 nm (n = 8). The average forward step size of myosin VI-992 was 54.2 ± 17.4 nm (n = 101), and the average backward step size of myosin VI-992 was −15.3 ± 4.9 nm (n = 3). The average forward step size of myosin VI-1050 was 60.4 ± 25.1 nm (n = 182), and the average backward step size of myosin VI-1050 was −21.7 ± 13.7 nm (n = 5). (B) Dwell time of stepping of full-length myosin VI. Dwell time histogram contains 221 steps of 60 full-length myosin VI dimers. The initial rise of histogram indicates the 60–0 nm steps. Histogram data fit very well to the convolution function based on kinetics of 60–0 nm step $P(t) = tk^2e^{-kt}$ (Yildiz et al., 2003). The rate constant was 1.12 s^{-1} at 40 μm ATP with R = 0.97.

in molar excess of actin was bound in rigor to actin filaments immobilized on a glass coverslip. ATP was then added to the solution, and the motility of labeled molecules was observed. Control experiments with labeled S1 constructs revealed that this procedure resulted in no motility; the molecules simply diffused away from the actin after addition of ATP. As shown in Figure 3, this technique revealed the presence of functional, processive dimers of the full-length molecule after the actin binding procedure. Importantly, the records in Figure 3

Table 3. Single Molecule Motility of Myosin VI Constructs as Assessed by FIONA (after Actin Saturation in Rigor)

Construct	Percentage of Molecules that Were Processive (Dimers)	Average Step Size (nm) (1/2 Observed Movement)	Average Run Length (μm)
S1 (MVI-839)	0	0	0
MVI-917	0	0	0
MVI-992	10	27.1 ± 8.7	0.6
MVI-1050	90	30.2 ± 12.6	0.9
Full length	15–30	27.6 ± 8.6	1.1
Zippered dimer	100	27.6 ± 9.8	0.3

(summarized in Table 3) show displacement of ~60 nm, which are nearly identical to our previously published records of the zippered dimer (Yildiz et al., 2004; Okten et al., 2004) and support a hand-over-hand mechanism. However, as was concluded with EM, the percentage of dimers formed with the full-length construct was much less than in the case of the truncated constructs with the cargo domain removed but with the high probability coiled coil present. In addition, full-length myosin VI showed a concentration dependence to motility. The percentage of moving to total molecules was less than 1% at 0.075 nM myosin, 7% at 0.75 nM, and 15% at 7.5 nM (Table 4). This demonstrates that close proximity of the monomers on the actin filament is necessary to allow dimerization.

Both MVI-992 and MVI-1050 moved as processive dimers after clustering on actin, with step size and run-length parameters similar to the full-length and zippered dimer constructs (Figure 3 and Table 3). However, in the case of MVI-992, this assay differed quantitatively from ATPase and EM assays in showing a low level of dimerization. As with the S1 construct, MVI-917 containing the low probability coiled coil failed to show motility, consistent with it remaining a monomer after clustering on actin (Table 3), in agreement with ATPase and EM data. Thus, the FIONA data also demonstrate that the predicted high probability coiled-coil region is necessary for dimerization.

Discussion

Taken together, all of the data are consistent with the suggestion that the predicted high probability coiled-coil region of myosin VI is capable of dimerizing the molecule but that it cannot itself efficiently initiate dimerization. By simply holding two monomers in close proximity (by tethering either end), we allow dimerization to occur, and this dimerization is made more efficient by removal of the cargo binding domain. As originally pointed out by Lister et al. (2004), the MVI-predicted coiled coil is

Table 4. Concentration Dependence of Full-Length Myosin VI Motility Using FIONA

Concentration	Percentage of Motility (Percentage of Moving Molecules/Total Molecules)
0.075 nM	< 1% (1/120)
0.75 nM	7% (13/197)
7.5 nM	15% (118/794)

unusual in its high content of charged amino acids and in the relatively few hydrophobic residues in core positions. Clearly, it is this highly charged region that is responsible for dimerization, as MVI-917, which lacks this region, is monomeric under all conditions. The region of low coiled-coiled probability (amino acids 840–917) that follows the IQ motif is likely an extension of the myosin VI lever arm, as proposed by Rock et al. (2005).

As recently noted by Knight et al. (2005), the predicted coiled-coil regions of myosin X and myosin VIIa, like that of myosin VI, are highly charged and contain few hydrophobic side chains in core positions. These authors demonstrated that myosin X, with its cargo binding domain removed, poorly self-initiates dimerization (~10% of total). This led the authors to propose that the hypothetical coiled coil might in fact be a stable, extended α helix (an extension of the myosin X lever arm). However, in the light of this study, it may be possible that like myosin VI, myosin X only forms dimers when monomers are bound in close proximity. Interestingly, the EM images of myosin X dimers (Knight et al., 2005) are similar to our native sequence myosin VI dimers in that they do not have a visible stalk attributable to the coiled coil. However, we do not feel that this implies that an antiparallel coiled coil has formed, as was suggested for myosin X (Knight et al., 2005), because the native myosin VI dimers and zippered dimers have identical properties in the single molecule assays (Table 3). From the EM images (Figure 2A, rows 2, 3, 5, and 7), it appears that the molecules have collapsed on the charged substrate, possibly due to the highly charged nature of the native coiled coil. However, even in images of full-length dimers that are positioned so that a C-terminal globular region (likely cargo binding region) is visible, a stalk is not visible as it is in the zippered dimer (Figure 2B). This may indicate that the coiled coil in the native dimers is much shorter than in our zippered dimmers but could also indicate collapse of the highly charged region onto the grid, because the zippered molecule in Figure 2B appears considerably longer than the native molecule.

Our data are also consistent with the cargo binding domain of myosin VI being capable of inhibiting dimerization, because in both the FIONA and EM studies (Tables 2 and 3), the same dimerization protocol (rigor binding to actin) generates more dimers when the cargo binding domain is removed (MVI-1050). Thus, a model emerges (diagramed in Figure 4) in which binding of myosin VI to cargo would serve two purposes. The first would be to alter the conformation of the cargo binding domain so that inhibition of dimerization would be removed. Second, either binding to a cargo that is itself dimeric or binding at high density on a vesicle surface would bring two full-length myosin VI monomers together, which would then initiate dimerization. The net result would be that cargo binding would lead to the creation of functional dimers of myosin VI.

Why regulate dimerization of myosin VI? It is possible that different cargos bind to different regions of the cargo binding domain such that some cargos promote dimerization and others do not, allowing it to function as either a dimer or a monomer, depending on its binding partner(s). Because myosin VI is the only myosin that clearly has been shown to traffic in the reverse direction, both configurations would function in the reverse direction. The fact that similar predicted coiled-coil domains are found in myosin X and VIIa (Knight et al., 2005) may imply that this ability to function as either a monomer or a dimer may not be a property limited to myosin VI but could represent a new paradigm for a subset of the myosin superfamily.

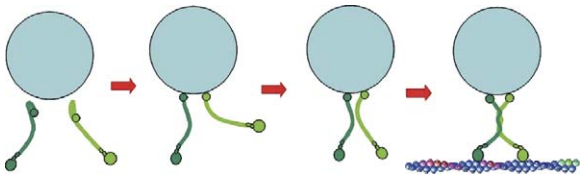

Figure 4. Cargo-Mediated Dimerization of Myosin VI

Our working model for myosin VI in a cell is that the full-length protein exists as a monomer if not bound to cargo. Binding of myosin VI monomers to cargo alters the conformation of the molecule, possibly exposing the high probability coiled-coil region. At the same time, close proximity of two monomers bound to cargo initiates dimerization. Once dimerized, the myosin VI can move the vesicle processively toward the minus end of an actin filament, using a hand-over-hand motion.

Although this is the first report of a regulated dimerization within the myosin superfamily of molecular motors, an analogous model has been put forward for *Unc104* of the kinesin superfamily. In that case, it was proposed that the coiled-coil domain forms a parallel coiled coil with itself, creating a monomer (Al-Bassam et al., 2003). Cargo binding was proposed to initiate dimerization by destabilizing the internal coiled coil and promoting coiled-coil formation with another monomer. In the case of myosin VI, we feel that it is more likely that the cargo binding domain directly interacts with the high probability coiled-coil region, trapping myosin VI as a monomer. Dimerization requires removal of this interaction via interaction with cargo.

Experimental Procedures

Protein Constructs, Expression, and ATPase Assays

A series of truncations of porcine myosin VI cDNA were generated. As depicted in Figure 1, C-terminal truncations were made corresponding to amino acids 839 (S1), 917, 992, and 1050. Each of these had a Flag tag (encoding GDYKDDDDK) appended to the C terminus to facilitate purification. Full-length myosin VI (amino acids 1–1273) had a Flag tag at the N terminus. As previously described (De La Cruz et al., 2001), a zippered dimer myosin VI construct was created by truncation at Arg-994, followed by a leucine zipper (GCN4; [Lumb et al., 1994]) to ensure dimerization. This sequence was followed by myc and Flag tags for motility assays and purification, respectively, as described previously (Sweeney et al., 1998). These constructs were used to create a baculovirus for expression in SF9 cells, as previously described (Sweeney et al., 1998). ATPase assays were performed as described (De La Cruz et al., 2001).

Labeling of Myosin VI for FIONA

Myosin VI has a single "IQ motif" (calmodulin binding site) following the motor domain and contains a unique insertion between the motor domain and IQ motif that has been shown to be a second binding site for calmodulin, but not an exchangeable one (Bahloul et al., 2004; Ménétrey et al., 2005). To selectively label only one of the two CaMs, we incubated labeled (Cy3) CaM with myosin VI and then raised and lowered the free calcium concentration, as previously described (Yildiz et al., 2004). This procedure resulted in 10%–20% labeling of the IQ motifs of myosin VI.

Dimerization Initiation Procedures

To hold myosin VI constructs in close proximity, myosin was bound either to a Flag antibody or to F-actin filaments in the absence of ATP. For antibody-initiated dimerization, an antibody to the C-terminal Flag epitope (Sigma, St. Louis. MO) was mixed in a ratio of 0.5:1 with myosin VI for 15 min on ice. A 2-fold excess of Flag peptide was next added for 1 hr, and the antibody was removed by centrifugation with protein A beads. Myosin remaining in the supernatant was used for ATPase or EM assays. Actin-initiated dimerization followed the same procedure as our normal purification protocol (Sweeney et al., 1998), which involved binding to phalloidin-stabilized F-actin in the absence of ATP. In this case, we saturated the actin by using a 20% excess of myosin over actin. The actin was pelleted, and the supernatant containing unbound myosin was removed. The remaining myosin was released from actin by the addition of 1 mM MgATP, and the actin was removed by centrifugation. The myosin in this supernatant was used for ATPase assays and EM.

EM

Myosin constructs were suspended and stored in a solution containing 50 mM KCl, 1 mM $MgCl_2$, 1 mM EGTA, 1 mM DTT, 10 mM imidazole (pH 7), and 50% (v/v) glycerol. Samples were diluted to a concentration of 60–120 μg/ml in the same solution, and 5–10 μl of each sample were sprayed on a freshly split mica surface, dried for 2 hr under vacuum, rotary shadowed with platinum at an angle of 7°, and replicated with carbon in a Balzers 410 freeze-fracture machine. Replicas were photographed in a Philips 410 electron microscope operating at 60 kV at a magnification of 75,300. The negatives were digitally scanned at 1000 ppi. The original images were obtained from areas at the edge of each droplet that showed distinct nonaggregated molecules and a clear background. A few of these micrographs were later discarded, because they mostly showed aggregated molecules. The individual profiles within each micrograph were classified into three categories based on an initial survey of the full-length myosin VI, which is monomeric. A single globular "structure," sometimes with a visible small tail, was considered to be monomeric myosin VI; two globular structures within a short distance of each other (~20 nm center to center) were classified as a single dimeric myosin. A number of other profiles, with variable and usually larger shapes, mostly aggregates of molecules, were classified as "unidentifiable" and were not included in the final counts. The molecules were deposited at a low density, so that the probability of classifying two closely spaced monomers as a single dimer was very low, as also shown by the data in Table 2. For each micrograph, the dimer frequency was calculated and expressed as a percentage of the total identified molecules. In order to verify the significance of these data, Student's t tests were conducted, using the number of micrographs as the sample size n.

Optics

All optics and data acquisition statistics used were previously described by Yildiz et al. (2004).

Acknowledgments

This work was supported by grants from the National Institutes of Health (AR44420, GM 068625, AR048931, and PO1-AR051174). We thank Anna Li, Xiaoyan Liu, and Bin Zong for technical assistance in preparing and assaying the recombinant proteins.

Received: September 10, 2005
Revised: November 4, 2005
Accepted: December 21, 2005
Published: February 2, 2006

References

Al-Bassam, J., Cui, Y., Klopfenstein, D., Carragher, B.O., Vale, R.D., and Milligan, R.A. (2003). Distinct conformations of the kinesin Unc104 neck regulate a monomer to dimer motor transition. J. Cell Biol. *163*, 743–753.

Bahloul, A., Chevreux, G., Wells, A.L., Martin, D., Nolt, J., Yang, Z., Chen, L.Q., Potier, N., Van Dorsselaer, A., Rosenfeld, S., et al. (2004). The unique insert in myosin VI is a structural calcium-calmodulin binding site. Proc. Natl. Acad. Sci. USA *101*, 4787–4792.

De La Cruz, E.M., Ostap, E.M., and Sweeney, H.L. (2001). Kinetic mechanism and regulation of myosin VI. J. Biol. Chem. *276*, 32373–32381.

Hasson, T., and Mooseker, M.S. (1994). Porcine myosin-VI: characterization of a new mammalian unconventional myosin. J. Cell Biol. *127*, 425–440.

Kellerman, K.A., and Miller, K.G. (1992). An unconventional myosin heavy chain gene from Drosophila melanogaster. J. Cell Biol. *119*, 823–834.

Knight, P.J., Thirumurugan, K., Yu, Y., Wang, F., Kalverda, A.P., Stafford, W.F., 3rd, Sellers, J.R., and Peckham, M. (2005). The predicted coiled-coil domain of myosin 10 forms a novel elongated domain that lengthens the head. J. Biol. Chem. *280*, 34702–34708.

Lister, I., Schmitz, S., Walker, M., Trinick, J., Buss, F., Veigel, C., and Kendrick-Jones, J. (2004). A monomeric myosin VI with a large working stroke. EMBO J. *23*, 1729–1738.

Lumb, K.J., Carr, C.M., and Kim, P.S. (1994). Subdomain folding of the coiled coil leucine zipper from the bZIP transcriptional activator GCN4. Biochemistry *33*, 7361–7367.

Ménétrey, J., Bahloul, A., Wells, A.L., Yengo, C.M., Morris, C.A., Sweeney, H.L., and Houdusse, A. (2005). The structure of the myosin VI motor reveals the mechanism of directionality reversal. Nature *435*, 779–785.

Morris, C.A., Wells, A.L., Yang, Z., Chen, L.Q., Baldacchino, C.V., and Sweeney, H.L. (2003). Calcium functionally uncouples the heads of myosin VI. J. Biol. Chem. *278*, 23324–23330.

Nishikawa, S., Homma, K., Komori, Y., Iwaki, M., Wazawa, T., Hikikoshi Iwane, A., Saito, J., Ikebe, R., Katayama, E., Yanagida, T., and Ikebe, M. (2002). Class VI myosin moves processively along actin filaments backward with large steps. Biochem. Biophys. Res. Commun. *290*, 311–317.

Okten, Z., Churchman, L.S., Rock, R.S., and Spudich, J.A. (2004). Myosin VI walks hand-over-hand along actin. Nat. Struct. Mol. Biol. *11*, 884–887.

Rock, R.S., Rice, S.E., Wells, A.L., Purcell, T.J., Spudich, J.A., and Sweeney, H.L. (2001). Myosin VI is a processive motor with a large step size. Proc. Natl. Acad. Sci. USA *98*, 13655–13659.

Rock, R.S., Ramamurthy, B., Dunn, A.R., Beccafico, S., Morris, C., Spink, B., Rami, B., Franzini-Armstrong, C., Spudich, J.A., and Sweeney, H.L. (2005). A flexible domain is essential for the large step size and processivity of myosin VI. Mol. Cell *17*, 603–609.

Sweeney, H.L., Rosenfeld, S.S., Brown, F., Faust, L., Smith, J., Xing, J., Stein, L.A., and Sellers, J.R. (1998). Kinetic tuning of myosin via a flexible loop adjacent to the nucleotide binding pocket. J. Biol. Chem. *273*, 6262–6270.

Wells, A.L., Lin, A.W., Chen, L.Q., Safer, D., Cain, S.M., Hasson, T., Carragher, B.O., Milligan, R.A., and Sweeney, H.L. (1999). Myosin VI is an actin-based motor that moves backwards. Nature *401*, 505–508.

Yildiz, A., Forkey, J.N., McKinney, S.A., Ha, T., Goldman, Y.E., and Selvin, P.R. (2003). Myosin V walks hand-over-hand: single fluorophore imaging with 1.5 nm localization. Science *300*, 2061–2065.

Yildiz, A., Park, H., Safer, D., Yang, Z., Chen, L.Q., Selvin, P.R., and Sweeney, H.L. (2004). Myosin VI steps via a hand-over-hand mechanism with its lever arm undergoing fluctuations when attached to actin. J. Biol. Chem. *279*, 37223–37226.